CARBURIZATION OF METALLIC PARTS IN AN ELECTROTHERMAL FLUIDIZED BED*

S. S. Zabrodskii, V. A. Borodulya,
R. L. Tofpenets, and G. G. Tyukhai

UDC 541.182.3:621.78

The carburization mechanism is presented for metallic components in an electrothermal fluidized bed; numerical results are presented.

Thermochemical treatment of metals in electrothermal fluidized beds enables one to accelerate surface treatment with various elements quite considerably [1]; we here present new experimental evidence that shows that this effect is obtained by combining various processes that will intensify the individual stages in the over-all process.

The method provides an unusually good improvement in modes of improving carburization, such as carburizator activation [2], surface temperature increase, and ion diffusion [2,3].

Carburization may be considered as consisting of several stages: supply of the carburizer to the surface of the component, activation, introduction of the carbon atoms into the metal, and finally transport of the ionized carbon atoms within the metal. It may be largely ineffective to intensify only some of these successive processes, because the neglected ones may represent the rate-limiting step.

If the material is made a cathode, each of the stages can be accelerated; the simplified model is that the carburizer is activated in microscopic arcs at the surface of the component, while the more rapid introduction of material into the metal occurs by electrical transport, and also as a result of surface heating of the metal near the discharges.

The temperature in one of these microscopic arcs may attain some thousands of degrees, but the temperature within the component of course falls rapidly away from such a point source. If such an arc were to burn for a prolonged time at one spot, one might get unacceptably high temperatures in the metal itself; the continual mixing in a fluidized bed will mean that the arc stays at one point only for a short time, and the surface of the component is not damaged.

It is difficult to say how long such an arc burns, because the fluctuations in the total current from the d.c. source do not give any clear idea about the frequency of occurrence and extension of these arcs. The oscillograms reveal pulsations with frequencies of 10^3-10^5 Hz. The frequency of striking and extinction at the surface may be much larger, because the pulsations actually recorded may well be only the low-frequency beats arising on account of addition of high-frequency primary pulsations in the arcs. On the other hand, the number of such arcs at the surface of the electrodes is much less than the total number within the volume of the layer, but general considerations would indicate that the arc duration must be very short. Arc extinction can be brought about not only by the escape from the electrode of a bunch of particles (which produces frequencies of the order of a few cycles per second) but also by slight displacement of the particles within a bunch. There are possible effects from the explosive expansion of the gas or vapor in the region of the arc, which can give the highly mobile light particles a large acceleration away from the electrode and thus very rapidly extinguish the arc.

---

*Paper read at the extended meeting on "Heat and Mass Transfer in Pseudofluidized Systems", 25-26 July, 1970.

Institute of Heat and Mass Transfer, Academy of Sciences of the Belorussian SSR, Minsk. Translated from Inzhenerno-Fizicheskii Zhurnal, Vol. 21, No. 1, pp. 120-126, July, 1971. Original article submitted October 26, 1970.

TABLE 1. Results on Carburization

Direct current

No.	t_{fl}, °C	t_{par}, °C	t, min	I, a	U, V	W_g at 20° C, m/sec	Graphite d, μm	Gas	Structure for specimens cooled in water (18° C)
1	800	Sample specimen between electrodes	15	52	50	0,036	50	Air	Thin surface layer with the structure of preeutectic cast iron
2	800		20	50	60	0,028	50	The same	Martensite structures in surface layer, ferrite network in core
3	890		10	50	55	0,027	127	"	Troostite + sorbite, core sorbite + ferrite
4	910		30	42	55	0,043	350	"	Thin decarburized layer, perlite and ferrite in core
5	960		5	36	75	0,06	127	"	Troostite + sorbite
6	960		10	37	80	0,053	"	"	Fine martensite needles in surface layer
7	960		15	32	80	"	"	"	Martensite structure in surface layer
8	995		30	45	60	0,043	350	"	Martensite + troostite
9	1000		10	50	75	0,02	127	"	Sorbite structure. Fine ferrite network in core
10	1000		15	42	75	0,043	350	"	Martensite structure
11	1000		15	42	75	"	"	"	Surface layer has structure of preeutectic concentration, core large needles of martensite + residual austenite. Some melting
12	1020		5	50	85	0,02	127	"	Surface layer with structure of preeutectic cast iron, martensite structure of core
13	1040		15	46	80	0,038	350	"	Thin surface layer with structure of preeutectic cast iron, then martensite + residual austenite. Martensite core structure, some melting
14	1040		30	46	65	0,03	"	"	Large needles of martensite + residual austenite, martensite structure of core
15	1100		3	47	90	0,015	127	"	Martensite structure, core sorbite and ferrite
16	1100		5	48	95	"	"	"	Martensite structure, core troostite + sorbite and ferrite
17	1100		15	50	100	0,02	"	"	Large martensite needles, with small ones in core
18	1200		30	30	60	0,015	300	"	Preeutectic cast-iron structure on melting side, martensite in core
19	800	930	30	37	60	0,082	300	"	Ferrite + martensite structure, proportion of ferrite increasing towards core
20	820	940	30	40	70	"	"	Tech. N_2	Martensite structure, ferrite network in core
21	870	920	60	34	40	0,15	"	Air	Martensite + ferrite structure throughout specimen
22	892	930	30	34	90	"	"	The same	Martensite structure, ferrite network in core
23	910	940	30	40	60	0,057	"	"	Martensite + residual austenite structure, troostite + sorbite in core
24	910	940	30	45	70	0,082	"	Nitrogen	Martensite structure, ferrite network in core
25	900	930	60	29	120	0,092	"	CO_2	Martensite + residual austenite structure, ferrite network appearing as core is approached
26	920	960	60	30	60	0,15	"	Air	Surface layer of martensite + residual austenite
27	930	975	30	38	100	0,082	"	The same	Martensite structure, ferrite network in core
28	960	1000	15	36	80	0,092	350	"	Martensite structure, sorbite in core
29	960	1000	15	31	80	"	"	"	Sorbite + ferrite structure
30	1000	1050	15	40	100	0,082	300	Nitrogen	Thin surface layer with structure of preeutectic cast iron, martensite in core, melting
31	1000	1050	25	42	90	0,092	350	Air	As 30, melted
32	1200	—	30	30	60	"	"	The same	As 30 and 31, melted

Provided the gas flow rate in the bed is sufficient to prevent arc damage to the component, one can in this way get a brief rise in the surface temperature by some hundreds of degrees near the point source of heat, which facilitates rapid diffusion of the carbon into the metal because of the marked temperature dependence of the diffusion coefficient [4]; for instance, the standard formula is

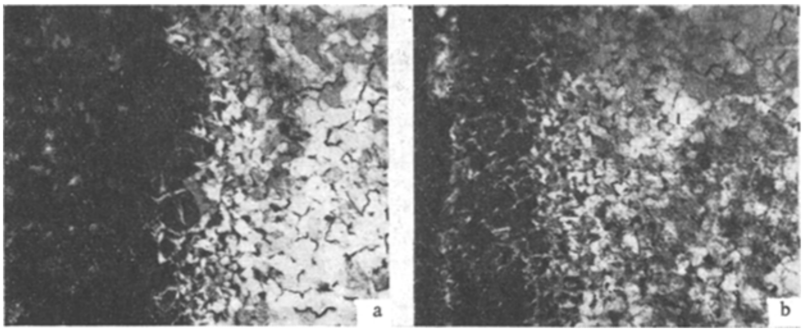

Fig. 1. Microstructure of Armco iron: a) side facing anode; b) cathode.

$$D_{c\to\gamma} = 0.064\exp\left(\frac{31350}{RT}\right).$$

Thermal diffusion also tends to accelerate the transport. All the carbon atoms in the metal are ionized [3], so diffusion of these into the part acting as cathode will be accelerated by the electric field. The primary entry of carbon into the metal is very greatly facilitated in our case not only by the local high temperature but also because the numerous microscopic arcs at the surface bring up sources of highly concentrated active carbon formed by burning and distillation of the graphite particles acting as anodes. The carbon atoms would appear to be ionized in these arcs and to move rapidly towards the metal under the electric field.

Another advantage of electrothermal fluidized beds is the scope for intensifying the diffusion of the carbon into the metal as a result of the higher temperatures [5], and also because the same mean surface temperature is accompanied by higher local temperatures near the arcs, which accelerates the diffusion because of the above-noted temperature dependence of the diffusion coefficient. The high heating rate provides a fine-grained structure [6] and improves the quality of the parts, as well as accelerating the diffusion [4, 7].

Table 1 gives results on carburization of specimens of steel type 3 (0.14–0.25% C) in such a fluidized bed, with the gas either air, carbon dioxide, or technical nitrogen. The tests were done at various gas flow rates with various particle diameters.

The carburization rate was greatly raised relative to that for gas carburization when a direct-current source was used, no matter whether the specimen was the cathode or lay between the electrodes. The carburized surface layer in most of the specimens contained about 0.6–0.8% C; at high temperatures and with long times (60 min) the specimen became completely saturated with carbon throughout the cross-section. There was no nonuniformity in structure and carbon content in specimens placed between the electrodes; evidently, in this case the general carbon transport into the specimen was not substantially interfered with by preferential entry from the side facing the cathode on account of the low current passing through the specimen.

However, a specimen of thick Armco iron (a piece of size 25 × 35 × 76 mm along the field line) clearly revealed differences in carburization rate in the anode and cathode regions after 15 min at 1000°C, as can be seen from the structure of the surface layer (Fig. 1). The side facing the anode had about 0.8% carbon (perlite structure), whereas on the other side it was only 0.5–0.6% (ferrite + perlite structure).

In routine operation, one can avoid differences in carburization either by turning the component or by periodically reversing the polarity of the electrodes.

If the specimen is the cathode, it carries more current, the electric field is stronger, and this and thermal diffusion result sometimes in so much more rapid entry of carbon that the internal parts actually contain more carbon than the surface. If there were signs of surface melting (Nos. 30–32 in Table 1), the carbon content rose to something approaching the eutectic value. This undesirable melting can be avoided even at high temperatures if one uses a gas flow rate that is not too low; of course, the available gas flow rate decreases as the graphite particle size is reduced.

If the specimen is the cathode, the current through the specimen and the electrical transport have accentuated effects. If alternating current replaces direct current, the carburization is much worse. Our tests show that there was no carburization at all on alternating current at 800-1000°C with comparatively large particles (300 μm). However, particles 127 μm in diameter and 950-1100°C produced a surface carbon concentration of 0.7-0.8% in 30 min, with 0.3-0.4% in the core. The carburization is better with small particles on account of the much larger number of arcs at the surface and the intensified diffusion; however, at present it is unclear what occurs when particles of 300 μm size are used, since then there was no appreciable carburization on ac.

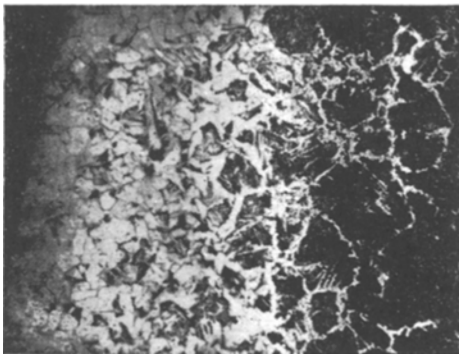

Fig. 2. Microstructure of Armcoiron sample made at $t_{fl} = 900°C$, $t_{par} = 1100°C$ and $\tau = 60$ min.

The following test shows that it is inadequate to accelerate only a single stage (electrical transport within the metal when the part is the cathode): the surface of a cylindrical specimen of steel type 45 was cut with a thread, and this was tightly screwed into a graphite container; under these conditions, the current the same as used in the main experiments was employed with the same hydrodynamic conditions in an attempt to carburize the specimen in an electrothermal layer of graphite with particles 127 μm in diameter. Each run lasted 35-60 min (Fig. 2). The microstructure revealed that the surface of the specimen had a decarburized layer, while between this layer and the core was a transition region with a gradually increasing carbon content, which rose to about 0.7% in the core. In this case, no carburization had occurred, because electrical transport of the carbon within the specimen to the core had occurred and the surface had not been supplied with carbon because there were no microscopic arcs between the surface and the graphite vessel.

These tests were done jointly with the Institute of Technical Physics, Academy of Sciences of the Belorussian SSR at the Minsk Tractor Works. A pilot-plant case-hardening apparatus was used with the ball-ended rods for the front suspension of the Belarus tractor, as well as for a pinion used in the transmission. The vehicle was operated at 970°C to obtain a carbon concentration of about 0.8% with a carburized layer 0.8-1.0 mm thick, which required 40 min. The surface of the metal showed no traces of scale. To obtain similar results in gas carburization would require 10-12 h.

NOTATION

D	is the diffusion on coefficient;
R	is the gas constant;
$C \rightarrow \gamma$	is the diffusion of carbon C into γ-phase;
U	is the voltage;
I	is the current;
W_g	is the linear velocity of gas flow;
t_{fl}	is the temperature of fluidized bed;
t_{par}	is the temperature of part;

LITERATURE CITED

1. S. S. Zabrodskii, V. A. Borodulya, R. L. Tofpenets, and G. G. Tyukhai, Izv. AN BSSR, ser. fiz. tekh., No. 4 (1970).
2. V. I. Prosvirin, Vestnik Metalloprom., No. 13 (1937).
3. I. N. Frantsevich and D. F. Kalinovich, Coll.: Powder Metallurgy and Strength of Materials [in Russian], issue 3, Izd. AN UkrSSR (1956).
4. A. N. Minkevich, Thermochemical Treatment of Metals and Alloys [in Russian], Moscow (1965).
5. S. S. Zabrodskii, V. A. Borodulya, R. L. Tofpenets, and G. G. Tyukhai, Coll.: Heat and Mass Transfer in Apparatus with Dispersed Systems [in Russian], Nauka i Tekhnika, Minsk (1970).
6. S. S. Zabrodskii, V. A. Borodulya, R. L. Tofpenets, and G. G. Tyukhai, Izv. AN BSSR, ser. fiz.-énergetika, No. 4 (1970).
7. I. N. Kidin, Physical Principles of Electrothermal Treatment of Metals and Alloys [in Russian], Metallurgiya, Moscow (1969).